3rd Specialty Conference on Disaster Prevention and Mitigation
3e Conférence spécialisée sur la prévention et la mitigation des désastres naturels

Montréal, Québec
May 29 to June 1, 2013 / *29 mai au 1 juin 2013*

Forecasting Drought via Bootstrap and Machine Learning Methods

Author(s) Anteneh Belayneh, Jan Adamowski. John Quilty, Bahaa Khalil, Bogdan Ozga-Zielinski

Abstract: This study explores the ability of machine learning techniques coupled with the bootstrap method to forecast drought conditions. The two machine learning techniques that were used were artificial neural networks and support vector regression. The potential of the bootstrap technique to reduce the uncertainty and develop reliable artificial neural network (ANN) and support vector regression (SVR) models was explored. The performance of the bootstrap-ANN (BANN) and bootstrap-SVR (BSVR) models were compared to traditional ANN and SVR models that do not use the bootstrap method. The Standard Precipitation Index (SPI) (in this case SPI 3, SPI 12 and SPI 24) was the drought index that was forecast using the aforementioned models. These SPI values represent short and long-term drought conditions and are analogous to agricultural and hydrological drought conditions, respectively. The performances of all models were compared using RMSE, MAE, R^2 and a measure of persistence. It was determined that the use of the bootstrap method reduced forecast uncertainties and improved the performance of the machine learning methods.

1 Introduction

Accurate drought forecasts are essential for effective water resource management as well as for effective crop management. There are many drought forecasting methods; however, as drought is a common phenomenon throughout the world, research is required to determine which forecasting method is most suitable for a given watershed. Drought forecasting models can either be physically based or data-driven in nature. Physical forecast models have the advantage of providing insight into catchment processes. However these models require many different types of data that are often difficult to obtain. Data driven models, in contrast are simpler to implement, require less data to develop and have rapid development times. Given these advantages, data driven models have found wide spread appeal in the field of hydrologic forecasting (Adamowski, 2008).

The main objective of this study was to compare the effectiveness of coupled bootstrap and machine learning techniques for drought forecasting in the Awash River Basin of Ethiopia. The standardized precipitation index (SPI) was the drought index forecasted in this study, as it is a good indicator of the variability of East African droughts (Ntale and Gan, 2003). SPI 3, SPI 12 and SPI 24 are forecast. SPI 3 is a good indicator of short-term drought conditions, while SPI 12 and SPI 24 are good indicators of long-term drought conditions. These SPI values at these time scales are likely tied to streamflows, reservoir levels, and even groundwater levels at the longer time scales, while SPI 3 is a good indicator of drought affecting agricultural systems.

1.1 The Standardized Precipitation Index (SPI)

The standardized Precipitation Index (SPI) was developed by McKee et al. (1993). The SPI index is based on precipitation alone making its evaluation relatively easy compared to other drought indices,

namely the Palmer Index and the crop moisture index (Cacciamani et al., 2007). A major advantage of the SPI index is that it makes it possible to describe drought on multiple time scales (Tsakiris and Vangelis, 2004; Mishra and Desai, 2006; Cacciamani et al., 2007). Given the fact that this study will explore forecasts of both short and long-term SPI values, this characteristic is especially useful. The SPI is also standardized which makes it particularly well suited for the comparison of droughts in different time periods and regions with different climates (Cacciamani et al., 2007). The SPI was selected for these reasons and it was also determined to be the best drought index for representing the variability in East African droughts (Ntale and Gan, 2002). Given the location of the Awash River Basin in East Africa, the choice of the SPI seems appropriate.

The computation of the SPI requires fitting a probability distribution to aggregated monthly precipitation series (3, 6, 12, 24, 48 months). The probability density function is then transformed into a normal standardized index whose values classify the category of drought characterizing each place and time scale (Cacciamani et al., 2007). SPI values can be categorized according to classes (Cacciamani et al., 2007). Normal conditions are established from the aggregation of two classes: $-1 < SPI < 0$ (mild drought) and $0 \leq SPI \leq 1$ (slightly wet). SPI values are positive or negative for greater or less than mean precipitation, respectively. Variance from the mean is a probability indication of the severity of the flood or drought that can be used for risk assessment (Morid et al., 2007). The more negative the SPI value for a given location, the more severe the drought.

1.2 Study area

In this study, the SPI was forecasted for the Awash River Basin in Ethiopia (Figure 1). Drought is a common occurrence in the Awash River Basin (Edossa et al., 2010). The heavy dependence of the population on rain-fed agriculture has made the people and the country's economy extremely vulnerable to the impacts of droughts. The mean annual rainfall of the basin varies from about 1,600 mm in the highlands to 160 mm in the northern point of the basin. The total amount of rainfall also varies greatly from year to year, resulting in severe droughts in some years and flooding in others. The total annual surface runoff in the Awash Basin amounts to some 4,900 $\times 10^6$ m^3 (Edossa et al., 2010). Effective forecasts of the SPI can be used for mitigating the impacts of drought that manifests as a result of rainfall shortages in the area. Rainfall records from 1970-2005 were used to generate SPI 3, SPI 12 and SPI 24 time series from each station.

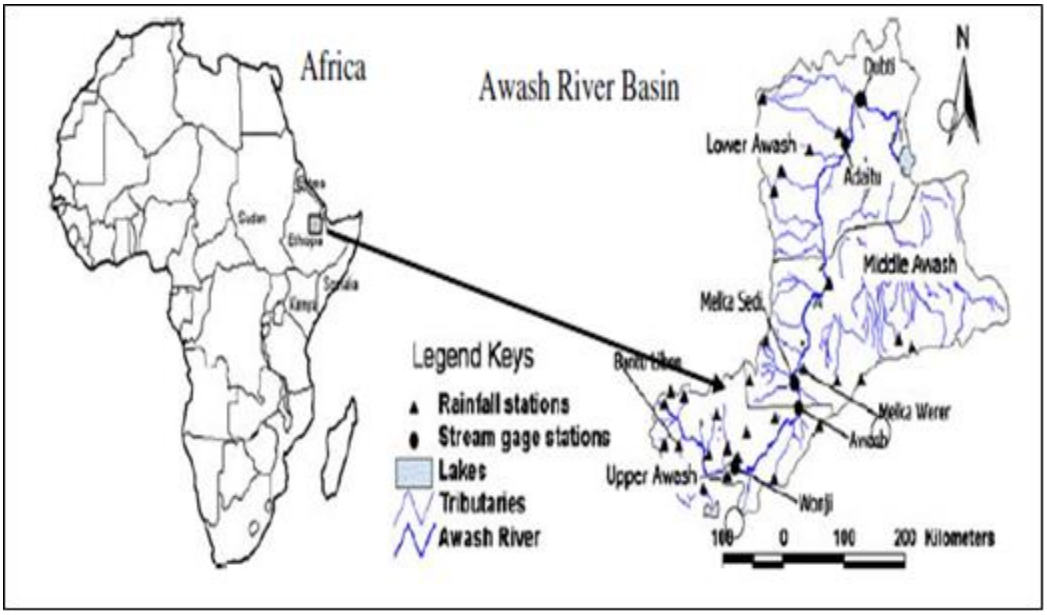

Figure 1. Awash River Basin (Source: Edossa et al., 2010).

2 Theoretical development

2.1 Artificial neural networks (ANNs)

All ANN models were created using MATLAB (R. 2012a). All inputs for ANN model development were standardized between 0 and 1. Each network was designed with the tangent sigmoid transfer function and the linear transfer function for the activation functions of the hidden and output layers, respectively. The Levenberg-Marquandt (LM) back propagation algorithm was used to train the network.

In this study, the number of neurons in the input and hidden layers were chosen to have between 1 - 9 neurons. Traditionally the number of hidden neurons for neural networks is selected via a trial and error method. However, a study by Wanas et al. (1998) empirically determined that the best performance of a neural network occurs when the number of hidden nodes is equal to log (*N*), where *N* is the number of training samples. Another study conducted by Mishra and Desai (2006) determined that the optimal number of hidden neurons is 2*n*+1, where *n* is the number of input neurons. In this study, the optimal number of hidden neurons was determined to be between log(*N*) and (2*n*+1). For example, if using the method proposed by Wanas et al. (1998) gave a result of 4 hidden neurons and using the method proposed by Mishra and Desai (2006) gave 7 hidden neurons, the optimal number of hidden neurons is between 4 and 7; thereafter the optimal number was chosen via trial and error. These two methods helped establish an upper and lower bound for the number of hidden neurons.

All ANN models were partitioned using the cross-validation technique where 80% of the data was used to train the model, 10% was used to validate the model, and the final 10% was used to test the network.

2.2 Support Vector Regression

Support vector machines (SVM), which were developed by Vapnik (1995) as a tool for classification and regression, embody the structural risk minimization principle, unlike conventional neural networks which adhere to the empirical risk minimization principle (Vapnik, 1995). All SVR models were created using the OnlineSVR software created by Parrella (2007), which can be used to build support vector machines for regression. The data was partitioned into two sets: a calibration set and a validation set. 90% of the data was partitioned into the calibration set while the final 10% of the data was used as the validation set. Unlike neural networks the data can only be partitioned into two sets with the calibration set being equivalent to the training and testing sets found in neural networks. All inputs and outputs were standardized between 0 and 1.

All SVR models used the nonlinear radial basis function (RBF) kernel. As a result, each WSVR model consisted of three parameters that were selected: gamma (γ), cost (C), and epsilon (ε). The γ parameter is a constant that reduces the model space and controls the complexity of the solution, while C is a positive constant that is a capacity control parameter, and ε is the loss function that describes the regression vector without all the input data (Kisi and Cimen, 2011). These three parameters were selected based on a trial and error procedure. The combination of parameters that produced the lowest RMSE values for the calibration data sets were selected.

2.3 Effect of bootstrap ensemble size

Ensemble artificial neural network models, namely BANN models, were designed in this study for the purpose of forecasting SPI3, SPI12, and SPI24 and to quantify and assess uncertainty surrounding the model predictions. In order to design BANN models with an optimal size of ensemble networks, RMSE versus ensemble size was plotted at SPI3 for Bati, Dubti, and Debre Zeit stations for their respective optimal ANN configurations as shown in Figure 2. The optimal ensemble network size was chosen when the RMSE value began to degrade in performance or remained approximately constant at an increase in ensemble size. The network architecture for each BANN model was adopted from the architecture of the best performing ANN at that particular station and SPI as reflected in Table 1(a-c).

As illustrated in Figure 2 the Bati station has the best performance in terms of RMSE for every ensemble network size. Each station shows little fluctuation in RMSE performance and each station can adequately

be represented by a BANN model only containing 10 ensemble networks. Since the purpose of this study is to design data-driven models for optimal performance, more than 10 ensemble networks were considered at each station, and the optimal ensemble networks sizes were chosen as 40, 50, and 60 for the Bati, Dubti, and Debre Zeit stations, respectively.

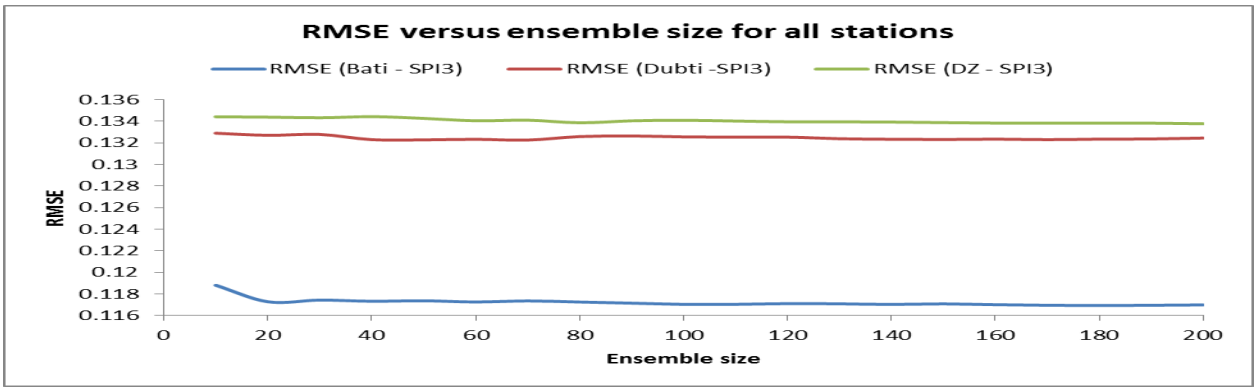

Figure 2 – Selection of ensemble networks in a BANN model for Bati, Dubti, and Debre Zeit stations

3 Results and Discussion

3.1 ANN model performance

The best performing ANN model for SPI3 occurs at the Bati station as shown in Table 1(a). The RMSE performance for the ANN model at the Bati station is measured as 0.0927 and is approximately 13-20% lower than Dubti and Debre Zeit stations, respectively and performing similarly for measures of R^2 and MAE.

As shown in Table 1(a) the best performing SPI12 ANN model occurs at the Bati station and is shown in Figure 3. The Bati SPI12 ANN model has an RMSE value of 0.0490 and it is at least 15% better performing than the other two stations for the same performance measure. The R^2 value for the Bati SPI12 ANN model was 0.8915 and shows high correlation between observed and predicted SPI12. The R^2 values for SPI12 models are more similar amongst stations than for SPI3 models, indicating that for longer SPI, the SPI calculation is less prone to noise and has better generalization ability for the respective models. The SPI12 ANN model for the Bati station reveals that extreme events of precipitation, or lack thereof, is equally generalized by the.

The best performing SPI24 ANN model occurs at the Bati station as shown in Table 1(a) with an RMSE value of 0.0464 and providing approximately 12% better performance with respect to RMSE measures at Dubti and Debre Zeit stations. There is a minor performance improvement at SPI24 compared to SPI12 for the ANN models at Bati station. The SPI24 ANN models show almost similar R^2 values between stations, indicating that increasing the SPI provides better generalization of all models and reduces the noise as well as the non-stationary nature of the data due to the notion that the onset of drought or increased precipitation becomes more evident as the time scale is increased. The very high R^2 values measured between observed and predicted SPI24 ANN models show the high degree of correlation between model inputs and outputs and provides better correlation than SPI12 models as expected.

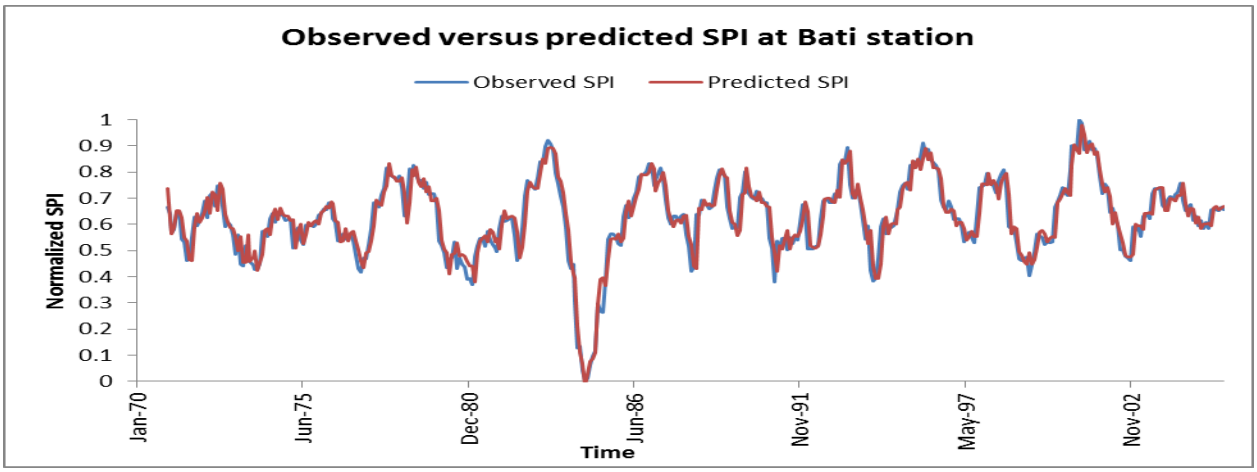

Figure 1 – SPI12 forecast results for the best performing ANN model occurring at Bati station

Table 1- (a) Performance results for the Bati station, (b) Performance results for the Dubti station, (c) Performance results for the Debre Zeit station.

(a)

	Entire Set			Test Set		
Model - Architecture - SPI	**R^2**	**RMSE**	**MAE**	**R^2**	**RMSE**	**MAE**
ANN - (8-7-1) - SPI3	0.6616	0.0927	0.0694	0.3307	0.1188	0.0954
BANN - (8-7-1) - SPI3				0.4571	0.1173	0.0917
ANN - (8-7-1) - SPI12	0.8915	0.0490	0.0362	0.8691	0.0499	0.0362
BANN - (8-7-1) - SPI12				0.8686	0.0539	0.0395
ANN - (6-9-1) - SPI24	0.9304	0.0464	0.0352	0.9524	0.0379	0.0305
BANN - (6-9-1) - SPI24				0.9170	0.0505	0.0372

(b)

	Entire Set			Test Set		
Model - Architecture - SPI	**R^2**	**RMSE**	**MAE**	**R^2**	**RMSE**	**MAE**
ANN - (8-9-1) - SPI3	0.5641	0.1068	0.0796	0.2977	0.1199	0.0900
BANN - (8-9-1) - SPI3				0.3310	0.1323	0.1008
ANN - (8-8-1) - SPI12	0.8777	0.0591	0.0409	0.8723	0.0635	0.0446
BANN - (8-8-1) - SPI12				0.8496	0.0654	0.0438
ANN - (9-7-1) - SPI24	0.9305	0.0528	0.0353	0.9055	0.0610	0.0404
BANN - (9-7-1) - SPI24				0.9104	0.0600	0.0374

(c)

	Entire Set			Test Set		
Model - Architecture - SPI	**R^2**	**RMSE**	**MAE**	**R^2**	**RMSE**	**MAE**
ANN - (9-7-1) - SPI3	0.5737	0.1153	0.0917	0.4729	0.1245	0.1034
BANN - (9-7-1) - SPI3				0.4245	0.1341	0.1057
ANN - (8-9-1) - SPI12	0.8991	0.0578	0.0446	0.8619	0.0705	0.0530
BANN - (8-9-1) - SPI12				0.8625	0.0676	0.0495
ANN - (9-8-1) - SPI24	0.9299	0.0530	0.0389	0.8500	0.0686	0.0534
BANN - (9-8-1) - SPI24				0.9146	0.0585	0.0422

3.2 BANN model performance

All outputs generated by the neural network for the BANN models are always part of the test set, as required by (Effron, 1979); whereas the optimal ANN configurations for a particular station and SPI was chosen on the overall performance and thus could have a sub-performing test set compared to training and validation sets. The best performing BANN model for the SPI3 occurs at the Bati station as shown in Table 1(a). The RMSE performance for the BANN model at the Bati station is measured as 0.1173 and is approximately 11-13% lower than Dubti and Debre Zeit stations, respectively and performing similarly for measures of MAE. There is a much larger variation in the R^2 measure amongst stations for the SPI3 BANN models; the Bati station shows a R^2 value 38% better performing than the Dubti station but only an 8% increase in R^2 performance over the Debre Zeit station. For the SPI3 models at Bati station the BANN model considerably improves the correlation between predicted and observed SPI3 at one-month ahead lead times over the ANN model by an increase of 38% in R^2 performance. The BANN model also provides a slight increase in RMSE and MAE over the ANN model for SPI3 at Bati station with performance measures of 0.1173 and 0.0917, respectively.

For SPI12 the best performing BANN model occurs at Bati station as shown in Table 1(a). The RMSE performance at Bati station for the BANN model at forecasting SPI12 only slightly outperforms Dubti and Debre Zeit stations in terms of R^2, RMSE, and MAE, indicating the increased performance of BANN models when forecasting SPI with larger time scales. All performance measures, R^2, RMSE, and MAE are nearly identical between the BANN model and ANN model test set for one-month ahead forecasting of SPI12 at Bati station with values of 0.8686, 0.0539, and 0.0395, respectively, for the BANN model. The BANN model at Bati station forecasts SPI12 very effectively as shown in Figure 5; while the mean ensemble predictions generally fit the observed time series well, any instances of increased precipitation and/or drought are covered by the upper and lower confidence bands. The Bati SPI12 BANN model is not as subjective to noise as the SPI3 BANN model at the same station and shows excellent generalization capabilities

Bati station has the best performing BANN model at forecasting as shown in Table 1(a). The RMSE performance at Bati station for the BANN model at forecasting SPI24 is similar to the SPI12 results, only slightly outperforming Dubti and Debre Zeit stations in terms of R^2, RMSE, and MAE, indicating the increased performance of BANN models when forecasting SPI with larger time scales. All performance measures, R^2, RMSE, and MAE are slightly underperforming for the BANN model when compared to the ANN model test set with values of 0.9170, 0.0505, and 0.0372, respectively.

The BANN model at Bati station forecasts SPI24 very effectively and improves upon the forecasting results for the SPI12 BANN model at the same station by lowering the variance among mean ensemble predictions and reducing the instances of over fitting and under fitting of the confidence bands. The Bati SPI24 BANN model is the least subjective to noise and shows the best generalization capabilities of all models. The two instances in October 1984 and April 1989 where the upper confidence band moderately overestimates a period of severe drought and moderate precipitation, respectively, in the Bati SPI12 BANN model is resolved with the Bati SPI24 BANN model as the model is able to effectively lower the variance in predictions at these locations in the time series.

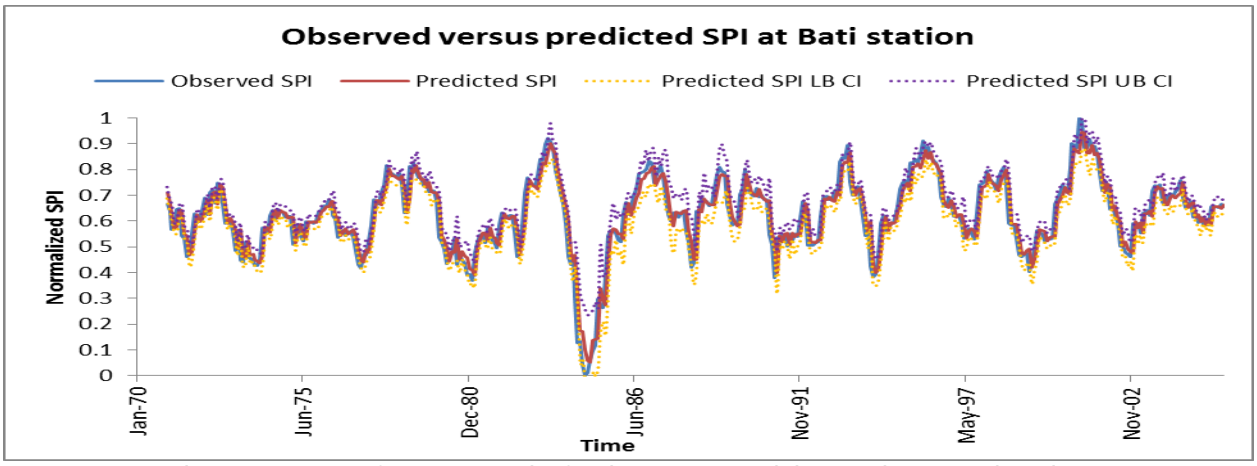

Figure 4 – SPI12 forecast results for the BANN model occurring at Bati station

For all stations and SPI the BANN models produce the most desirable results of the two modeling approaches. The BANN models adequately match in performance the best ANN models and in most cases improve upon the generalization ability of the single ANN model for a given neural network architecture. The SPI3 dataset is the most prone to noise and provides the lowest R^2, RMSE, and MAE performance measures. The BANN models greatly improve the reliability of forecasting SPI3 as the upper and lower confidence bands generally account for drastic changes in the SPI values and estimate periods of increased precipitation or drought adequately. The BANN models provide increased reliability and considerably reduce the variance. The SPI24 BANN models have the lowest variance amongst all SPI indices and are able to overcome predictive accuracy issues that burden SPI3 and SPI12 at noisy periods in the input series. Lastly, as the SPI extends to a large time scale, the variance of the BANN models continues to decrease and thus supports the inkling that SPI with wider time scales are less prone to noise and are thus more accurately forecasted with data-driven approaches such as BANN modeling techniques that provide uncertainty assessments.

3.3 SVR model performance

The SVR models in this study performed similarly for SPI 3 forecasts. The best model results according to RMSE are at the Bati station, while the Debre Zeit station exhibits the best results in terms of R^2 and MAE, respectively. The RMSE at the Bati station was 0.202, which outperformed the other stations by up to 7.76%. The results at the Debre Zeit station are up to 8.5% higher than the other stations in terms of R^2 and 2.94% lower in terms of MAE.

The Bati station exhibited the best results for SPI 12 forecasts in terms of R^2, MAE and RMSE as shown in Table 2(a). The R^2 of the Bati model was 0.8431, the RMSE was 0.0831 and the MAE was 0.0620. The results of the Bati model were between 5.76-7.3% better than the results from the other two stations. The forecast results for SPI 12 at the Bati Station are exhibited in Figure 5. While the model accurately mimics the periods of drought throughout the time series, there is a lag between observed and predicted values.

The SVR model that had the best results for SPI 24 was the model from the Debre Zeit station, as shown in Table 2 (c). The results from this model exhibited the lowest values of RMSE and MAE, respectively and were between 5.88% and 6.97% lower than those exhibited by other models. The SVR model at the Bati station exhibited the highest results in terms of R^2, a value of 0.8900.

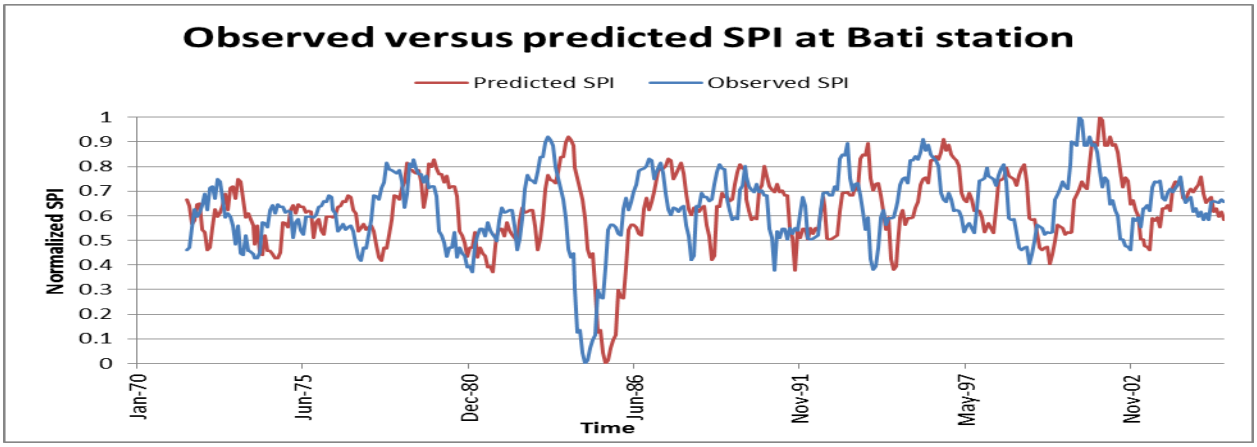

Figure 5 – SPI12 forecast results for the best performing SVR model occurring at Bati station

The results of the SVR models, for each SPI value forecasted, exhibit similar results. The differences between models decrease for SPI 12 and subsequently SPI 24 indicating an increase in generalization ability with longer term SPI values. The high R^2 values exhibited in all the models indicates a high correlation between the predicted and observed SPI values. The SPI24 models show very similar R^2 values between stations, indicating that increasing the SPI provides better generalization of all models and reduces the noise as well as the non-stationary nature of the data due to the notion that the onset of drought or increased precipitation becomes more evident as the time scale is increased.

Table 2- (a) Performance results for the Bati station, (b) Performance results for the Dubti station, (c) Performance results for the Debre Zeit station.

(a)

Model-(γ,C,ε)-SPI	R^2	RMSE	MAE
SVR–(0.65, 91, 0.008)–SPI3	0.5358	0.2020	0.1990
BSVR-(0.8, 96, 0.008)-SPI3	0.4732	0.2011	0.1624
SVR-(0.55, 85, 0.004)-SPI12	0.8431	0.0831	0.0620
BSVR-(0.05, 93, 0.004)-SPI12	0.8631	0.1405	0.1308
SVR-(0.04, 98, 0.008)-SPI24	0.8900	0.0958	0.0804
BSVR-(0.05, 88, 0.01)-SPI24	0.9147	0.0901	0.0801

(b)

Model-(γ,C,ε)-SPI	R^2	RMSE	MAE
SVR–(0.9, 92, 0.008)–SPI3	0.5883	0.2190	0.2040
BSVR-(0.6, 90, 0.008)-SPI3	0.4391	0.1960	0.1628
SVR-(0.05, 93, 0.003)-SPI12	0.8396	0.1054	0.0851
BSVR-(0.08, 97, 0.05)-SPI12	0.8136	0.0943	0.0515
SVR-(0.08, 97, 0.05)-SPI24	0.8371	0.0410	0.0400
BSVR-(0.09, 90, 0.007)-SPI24	0.9045	0.0672	0.0583

(c)

Model-(γ,C,ε)-SPI	R^2	RMSE	MAE
SVR–(0.5, 95, 0.009)–SPI3	0.6400	0.2080	0.1980
BSVR-(0.07, 87, 0.004)-SPI3	0.4812	0.1904	0.1579
SVR-(0.4, 96, 0.006)-SPI12	0.8058	0.0886	0.0640
BSVR-(0.4, 90, 0.008)-SPI12	0.8244	0.1259	0.0971
SVR-(0.6, 93, 0.008)-SPI24	0.8292	0.0922	0.0639
BSVR-(0.8, 98, 0.008)-SPI24	0.8658	0.1083	0.0874

3.4 BSVR model performance

The BSVR model that provided the best forecasts for SPI 3 was the model at the Debre Zeit station. The model results had the highest value for R^2 and the lowest values for both RMSE and MAE, respectively. The RMSE and MAE values from the Debre Zeit station were between 1-5% lower than the results at the other stations. Compared to the results of the SVR models for SPI 3, the BSVR models at all stations have slightly better results in terms of RMSE and MAE, respectively. The correlation between observed and predicted models is higher in SVR models than in BSVR models for SPI 3.

The BSVR forecast results for SPI 12 were very similar to the results from SVR models. The model at the Dubti station had the best forecast results in terms of RMSE and MAE, with results of 0.0943 and 0.0515 respectively. As in the results for SVR models, the results in BSVR models were more accurate for longer term SPI values. This trend is especially evident in the improvement in forecast results as exhibited by R^2. The correlation between observed and predicted values is much higher for forecasts of SPI 12 and SPI 24 than for SPI 3. In addition, the RMSE and MAE values are lower for forecasts of SPI 12 and SPI 24 compared to SPI 3. Figure 6 indicates that the BSVR models reduce the time step error exhibited between observed and predicted values, as compared to SVR models.

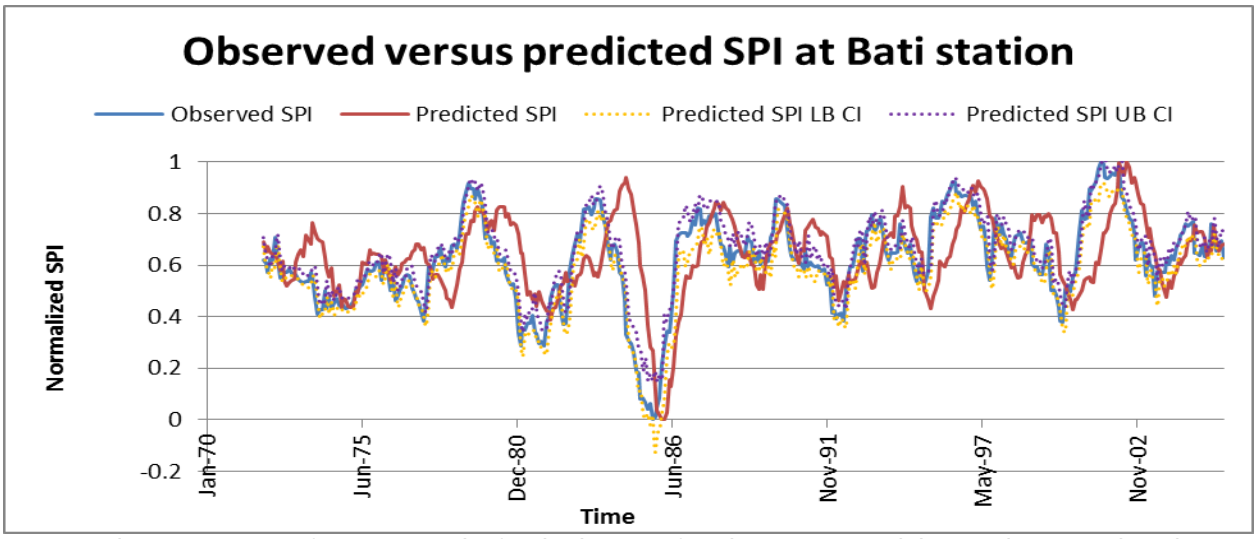

Figure 6 – SPI12 forecast results for the best performing BSVR model occurring at Bati station

4 Discussion

The ability of machine learning techniques coupled with a bootstrap technique to forecast the SPI 3, SPI 12 and SPI 24 was investigated in this study. This study found that the bootstrap technique improved drought forecast results for both ANN and SVR models. The results from SVR models exhibited a time lag between observed and predicted values. This time step error was reduced with the use of the bootstrap technique. The results for SPI 12 and SPI 24 were much better than the results for SPI 3 as the long term SPI values are less susceptible to noise.

Acknowledgements

An NSERC Discovery and FQNRT New Researcher Grant held by Dr. Jan Adamowski were used to fund this research. The data was obtained from the Meteorological Society of Ethiopia (NMSA). Their help is greatly appreciated

References

Adamowski, J. 2008. Development of a Short-term River Flood Forecasting Method for Snowmelt Driven

Floods Based on Wavelet and Cross-Wavelet Analysis. *Journal of Hydrology*, 353:247-266
Cacciamani, C., Morgillo, A., Marchesi, S., Pavan, V. 2007. Monitoring and Forecasting Drought on a Regional Scale : Emilia-Romagna Region. *Water Science and Technology Library* 62(1): 29-48
Desalegn, C., Babel, M.S., Das Gupta, A., Seleshi, B.A., Merrey, D. 2006. Farmers' Perception about Water Management Under Drought Conditions in the Awash River Basin, Ethiopia. *International Journal of Water Resource Development* 22(4):589–602.
Edossa, D.C., Babel, M.S., Gupta, A.D. 2010. Drought Analysis on the Awash River Basin, Ethiopia, *Water Resource Management* 24: 1441-1460
Efron, B. 1979. Bootstrap Methods: Another Look at the Jackknife. *Annals of statistics* 7: 1-26
Efron, B and Tibshiranim J. 1993. *An Introduction to the Bootstrap*. Chapman and Hall, London, UK
Kim, T., Valdes, J.B. 2003. Nonlinear Model for Drought Forecasting Based on a Conjunction of Wavelet Transforms and Neural Networks. *Journal of Hydrologic Engineering* 8: 319-328
Kisi, O., Cimen, M. 2011. A Wavelet-support Vector Machine Conjunction Model for Monthly Streamflow Forecasting. *Journal of Hydrology* 399: 132-140
McKee, T.B., Doesken, N.J., Kleist, J. 1993. The Relationship of Drought Frequency and Duration to Time Scales. *Paper Presented at 8th Conference on Applied Climatology. American Meteorological Society*, Anaheim, CA
Mishra, A. K. and V. R. Desai 2006. Drought Forecasting using Feed-forward Recursive Neural Network *Ecological Modelling* 198(1-2): 127-138
Morid, S., Smakhtin, V., Bagherzadeh, K. 2007. Drought Forecasting using Artificial Neural Networks and Time Series of Drought Indices. *International Journal of Climatology* 27(15): 2103-2111
Ntale, H. K. and T. Y. Gan 2003. Drought Indices and their Application to East Africa. *International Journal of Climatology* 23(11): 1335-1357.
Parrella, F. 2007. Online Support Vector Regression. Master Thesis, University of Genoa.
Tiwari, M.K., Chatterjee, C. 2010. Development of an Accurate and Reliable Hourly Flood Forecasting Model using Wavelet-bootstrap-ANN (WBANN) Hybrid Approach. *Journal of Hydrology* 394: 458-470.
Tsakiris, G., Vangelis, H. 2004. Towards a Drought Watch System based on spatial SPI. *Water Resource Management* 18 (1): 1-12
Vapnik, V. 1995. The Nature of Statistical Learning Theory, Springer Verlag, New York, USA.
Wanas, N., Auda, G., Kamel. M.S., Karray., F. 1998. On the Optimal Number of Hidden Nodes in a Neural Network. *Proceedings of the IEEE Canadian Conference on Electrical and Computer Engineering*. 918–921